

NRL Report 7257

An Experiment on Transmission Loss and Fluctuations of 3-kHz Sound in Shallow Water

ANDREW L. FABER

*Shallow Water Surveillance Branch
Acoustics Division*

April 13, 1971



NAVAL RESEARCH LABORATORY
Washington, D.C.

Approved for public release; distribution unlimited.

CONTENTS

Abstract	ii
Problem Status	ii
Authorization	ii
Acknowledgment	ii
INTRODUCTION	1
EQUIPMENT	2
Source	2
Receiving Ship Instrumentation	2
NRL PROCESSING	2
RESULTS	4
Pulse Data (Towed Run)	4
CW Data	9
CONCLUSIONS	20
APPENDIX A—Digitization and Computer Processing	21
APPENDIX B—Power Spectrum Techniques	23
REFERENCES	25

ABSTRACT

This experiment investigated certain aspects of the 3-kHz sound field produced by a source at middepth in shallow water off Panama City, Florida. The sound-speed profile consists of a weak surface channel in the upper half of the water column and a strong negative gradient in the lower half. A two-layer normal-mode model predicts that due to the source placement and high directivity, modes of lower order than the fourth or higher order than the twelfth should not be significantly excited. The prediction concerning the absence of the second and third modes tends to be supported by the amplitude distribution over depth observed at ranges of 15 to 27 km during a towed-hydrophone run (the data are inconclusive concerning the first mode). In the second part of the experiment the anchored receiving ship recorded about 48 hours of CW signals at each of two ranges: 7.0 km and 27.6 km. Over the total time span of the data the amplitude fluctuations of signals received on three hydrophones at different depths were observed to be weakly correlated, and there was some indication of variation at the tidal frequency for the 7.0-km data. On a shorter time scale, semiperiodic fluctuations at periods from 30 sec to 30 min occurred at times during these runs. Spectra of the signal amplitudes display strong peaks at the surface wave and swell frequencies, with the effect being somewhat greater at the shorter range, and with all three hydrophones having at any time similar fluctuation spectra.

PROBLEM STATUS

This is a final report on one phase of two NRL Problems. NRL Problem S01-33 is closed, and NRL Problem S01-45 is continuing.

AUTHORIZATION

Experiment done under NRL Problem S01-33,
Projects SF 11-552-001-8621 and RF 05-552-401-5257

Report issued under NRL Problem S01-45,
Projects SF 11-552-001-14275 and RF 05-552-404-5350

ACKNOWLEDGMENT

The experiment described in this report was planned and conducted by the Ocean Acoustics Branch under the direction of A.T. McClinton, R.W. Chrisp, and W.M. Lawson, Jr. As a result of subsequent reorganization of the Acoustics Division, most of the personnel connected with the experiment became part of the Systems Engineering Staff. A portion of the 117 reels of analog magnetic tape data acquired during the experiment has been reduced and analyzed by the Shallow Water Surveillance Branch and is the subject of this report.

Manuscript submitted February 2, 1971.

AN EXPERIMENT ON TRANSMISSION LOSS AND FLUCTUATIONS OF 3-KHz SOUND IN SHALLOW WATER

INTRODUCTION

An experiment was conducted during the period July 29 through August 11, 1968, in the Gulf of Mexico to get a preliminary look at the signal field in this shallow water area as a function of range, receiver depth, and time. A highly directional 3-kHz source was deployed from a fixed tower, a Naval Ship Research and Development Laboratory, Panama City, facility known as Stage I. This tower stands in 31 m of water approximately 20 km offshore from Panama City, Florida, at $30^{\circ}00'06''\text{N}$ and $85^{\circ}54'02''\text{W}$ (Fig. 1). All acoustic data were taken along a 225-degree bearing line from Stage I; the hard sand bottom is smooth and gently sloping, having a depth of 31 m at Stage I and 40 m at a range of 28 km.

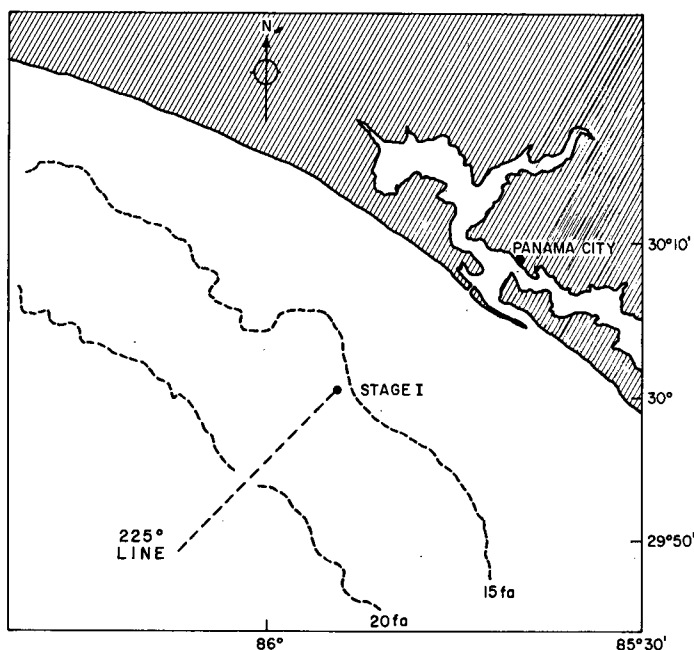


Fig. 1 - Location of the experiment
off Panama City, Florida

Two kinds of acoustic data were taken during this experiment. At the beginning of the experiment the receiving ship, the USNS *Gilliss* (T-AGOR-4), towed a vertical array of 10 hydrophones from 1.6 km to 27 km from the tower. This was repeated in the reverse direction from 56 km to 1.5 km at the end of the experiment. During these runs pulses of 1 sec and 40 ms duration were transmitted by the source. In the interval between the two towed runs the ship anchored successively at ranges of 7.0 km, 14.3 km, and 27.6 km. At each station approximately 48 hours of 3-kHz CW signals were received on a vertical

three-hydrophone array. The ship also anchored briefly at 65 km, but no signals were observed. The prevailing sound-speed profile for all of the runs consisted of a weak surface channel in the upper half of the water column and a strong negative gradient in the lower half.

Pulse data from four of the hydrophones (more at certain ranges) for the first towed run have been reduced and are reported here, along with some results from the CW signals received at the 7.0-km and 27.6-km stations. Due to a malfunction of the source, the source level for the second towed run was greatly reduced. Data from that run have not been analyzed.

EQUIPMENT

Source

The acoustic source consisted of a cylindrical transducer mounted in a 3-m-diameter parabolic reflector (Gregory, 1969). Throughout this experiment the source was positioned at a nominal depth of 15.2 m, which is approximately the middepth of the water column.

The source was highly directional, with a front lobe 10 degrees wide, vertically and horizontally, at the half-power points. The source level used in determining transmission loss during the towed run was 126.8 dB re 1 dyne/cm² at 1 meter. The towed run was terminated when the source malfunctioned, and for the remainder of the experiment the source was run at reduced power with a source level of approximately 103 dB re 1 dyne/cm² at 1 meter for the 7.0-km-range station, and 110 dB for the 27.6-km-range station.

Receiving Ship Instrumentation

During the towed run a ten-element hydrophone string with 3 m separation between hydrophones and a heavy weight at the lower end was suspended from a U-frame at the stern of the ship. The top hydrophone was held at the surface out to a range of 5.6 km, after which deepening water allowed it to be lowered to 3 m below the surface, with the bottom hydrophone then at 30 m. The average ship's speed during this run was 0.9 knot; the cable where entering the water was nearly vertical. Signals from the ten hydrophones were amplified, filtered (5% total bandwidth at the half-power points), and recorded on ten frequency-modulated channels of an analog tape recorder at 15 ips. Block diagrams of the instrumentation for the towed run and for the CW range stations are shown in Fig. 2.

At each anchored station, three hydrophones were suspended in the water column and connected to the ship by long (up to 240 m) cables, to which were attached empty plastic bottles for flotation. Fixed 40-dB preamplifiers were inserted in the hydrophone lines near the surface to present a low impedance for the long cable runs. At the ship the signals were again amplified, filtered, and recorded on analog magnetic tape, in this case in the "direct" mode at 3-3/4 ips. The nominal submerged depths of the hydrophones at the two anchored stations are given in Table 1.

NRL PROCESSING

Of the towed-hydrophone data, only the 1-sec-duration pulses were analyzed. Although these were transmitted every 20 sec, in the processing every other pulse was used, giving an effective pulse interval of 40 sec.

The pulses were played back at 60 ips (sped up by a factor of 4) detected by a half-wave diode detector with a rise time constant of 0.075 ms and decay time constant of 5 ms,

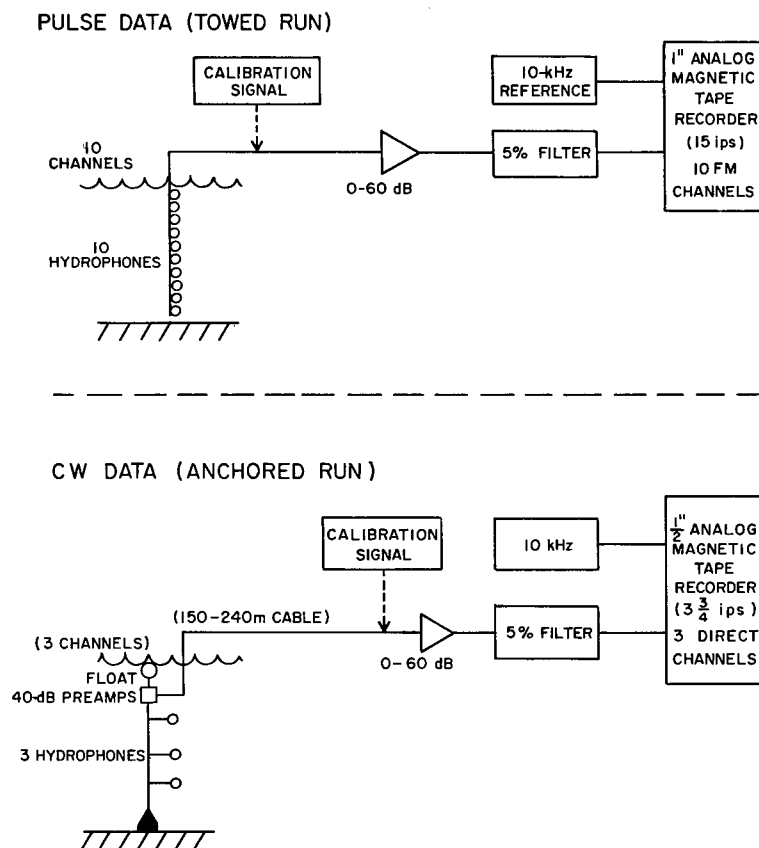


Fig. 2 - Receiving ship instrumentation

Table 1
Nominal Depths of the Hydrophones
at the Anchored Stations

Range (km)	Nominal Water Depth (m)	Channel No.	Nominal Hydrophone Depth (m)
7.0	33.6	1	6.7
		2	16.2
		3	25.3
27.6	40.3	1	7.6
		2	19.8
		3	32.0

and "integrated" on a voltage-to-frequency converter and electronic counter. By comparing the count with that produced by a calibration sine wave put on the tape when the pulses were recorded, the average rms voltage level of the pulse at the input to the tape recorder was determined. These values were then converted to propagation loss using the known source level and hydrophone sensitivities.

The CW data were digitized using the NAREC computer at NRL. The analog data were played back at 60 ips (sped up by a factor of 16), amplified, and detected using the same diode detectors as for the pulse data; then the three hydrophone channels were sampled sequentially at a real-time rate of 12.5 samples per second. The sampling rate was controlled by the 10-kHz reference frequency recorded on the analog tapes. The output of the 10-bit-plus-sign analog-to-digital converter was then written out on digital tapes, with time and tape identification at appropriate intervals. No analog filtering was used. All further processing of the CW data was carried out on the NRL CDC 3800 computer.

RESULTS

Pulse Data (Towed Run)

The towed-hydrophone run commenced at 1400 local time (central daylight time) on July 29, 1968, and ended at 0630 the next morning, for a total duration of 16-1/2 hours. During this interval no sound-speed profiles were measured directly; however, seven expendable-bathymograph records were obtained (Fig. 3). The bathymographs are quite similar in character to those obtained during the later anchored runs, at which time velocimeter casts were also taken. Therefore an average of the sound-speed profiles obtained directly during the first anchored run (see Fig. 8) is assumed to have been present during the towed run.

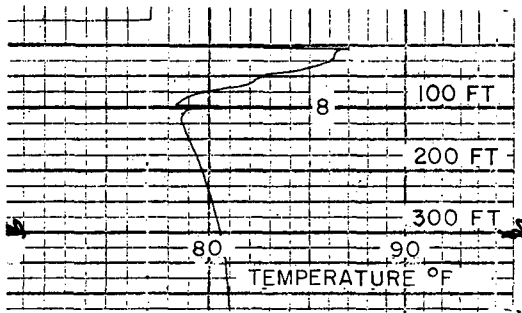
Signals received on four of the ten receiving hydrophones have been processed to yield transmission loss as a function of range (Fig. 4). As mentioned earlier, alternate 1-sec pulses at each depth were analyzed. Each dot in Fig. 4 represents the transmission loss for the average amplitude of three of these pulses, i.e. an average over 120 seconds, during which time the ship moved about 60 m. Gaps in the data were caused mainly by magnetic-tape problems, primarily connected with excessive oxide flaking from the tapes. Figure 5 shows the transmission loss smoothed in range; in this figure each point represents the transmission loss of the average signal received over an interval of 0.9 km.

We can gain a qualitative understanding of the propagation by considering the nature of the normal modes that should exist under the given sound-speed profile. The sound field at long ranges in shallow water can be written as a sum of normal modes of the acoustic duct (see Tolstoy and Clay, 1966, for a complete description of normal-mode theory applied to underwater sound). Upon solving the acoustic wave equation in the duct, one finds that the pressure $p(r, z)$ at range r and depth z can be written as

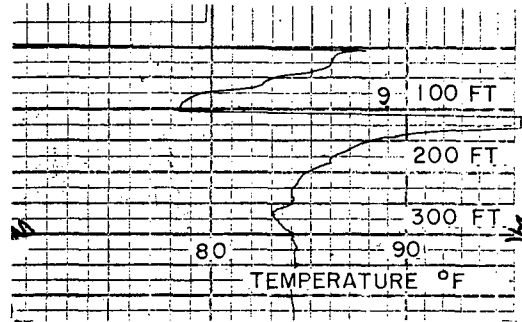
$$p(r, z) = \sum_m C_m(r) \phi_m(z) \phi_m(z_0), \quad (1)$$

where ϕ_m is the solution to the wave equation in the vertical dimension for the m th mode, z_0 is the source depth, and $C_m(r)$ gives the range dependence for each mode. A normal-mode computer program described in an earlier report (Ferris, Ingenito, and Faber, 1970), which can accommodate an arbitrary sound-speed profile in the water and which assumes a single-layer fluid bottom of density ρ and sound speed c , was used to solve the wave equation and produce the normalized mode amplitude functions $\phi_m(z)$, the first ten of which are shown in Fig. 6.*

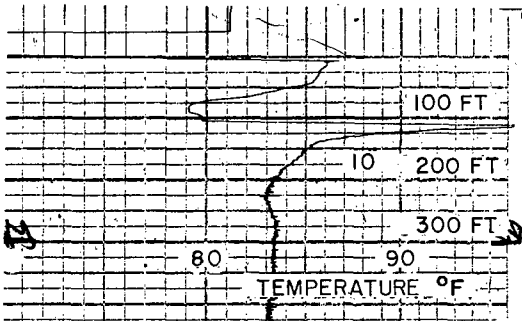
*The sound speed profile used was the "average" profile discussed. Values of ρ (1.85 g/cm³) and c (1589 m/sec) were obtained previously by a bottom-reflection technique (Ferris and Kuperman, 1970).



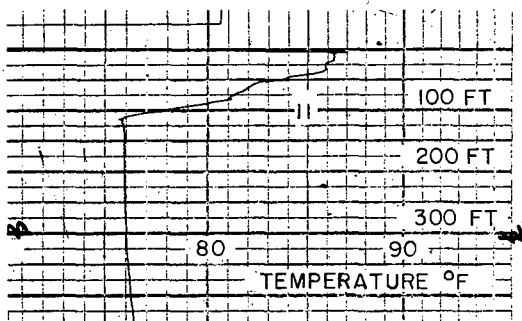
(a) 1400, July 29



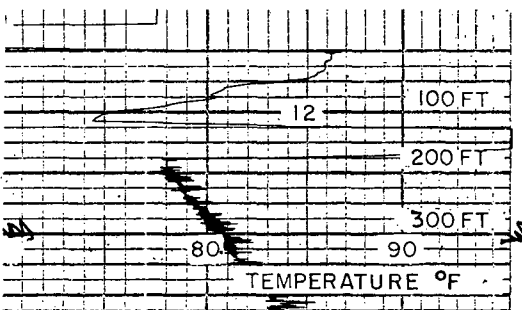
(b) 1700, July 29



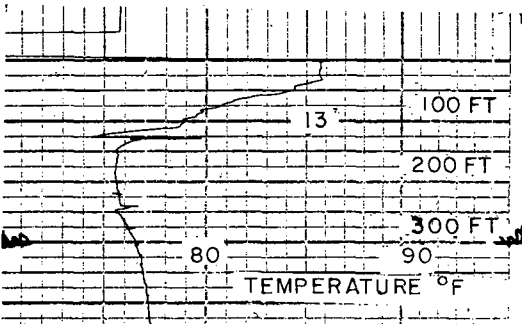
(c) 2000, July 29



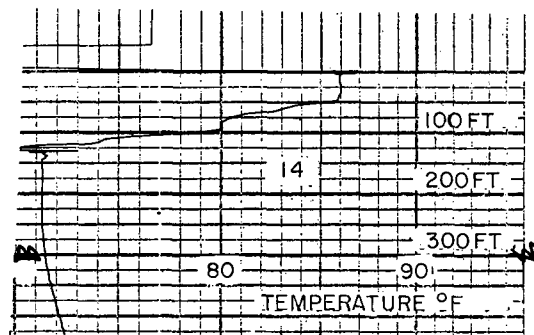
(d) 2300, July 29



(e) 0200, July 30

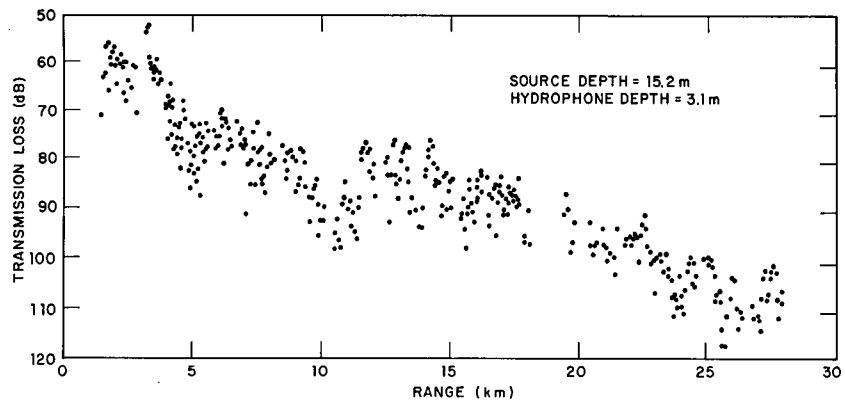


(f) 0500, July 30

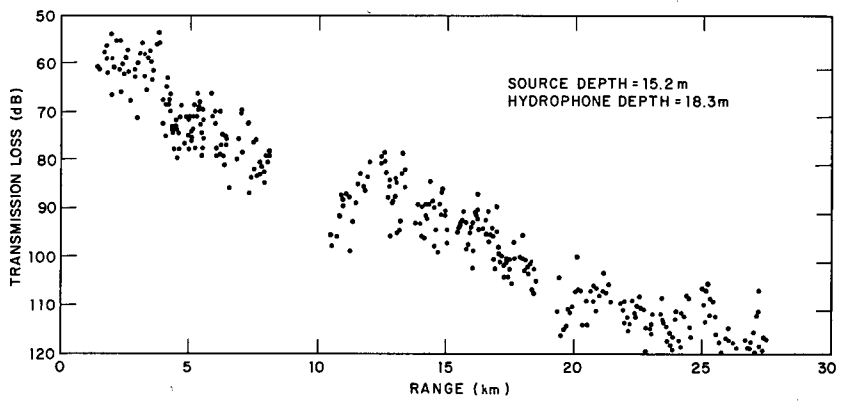


(g) 0800, July 30

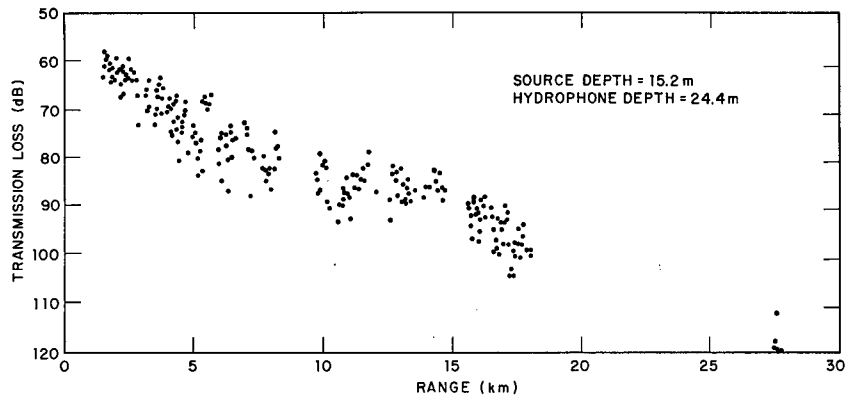
Fig. 3 - Bathythermograph traces obtained during the towed run



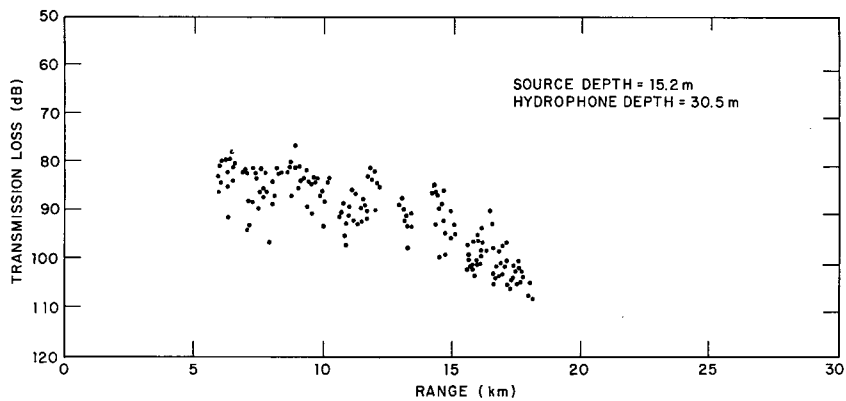
(a) Hydrophone 3.1 m deep



(b) Hydrophone 18.3 m deep



(c) Hydrophone 24.4 m deep



(d) Hydrophone 30.5 m deep

Fig. 4 - Transmission loss as a function of range for the signals received on four hydrophones during the towed run

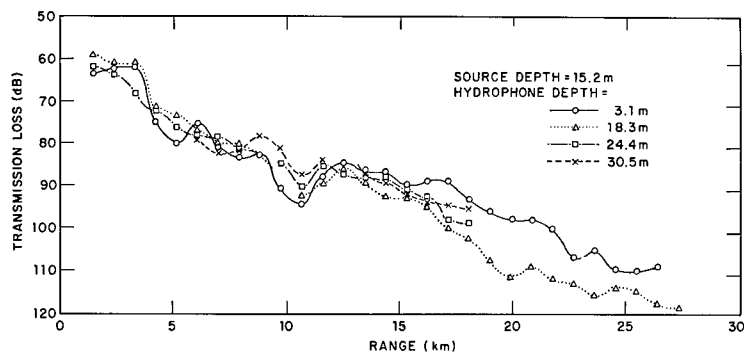


Fig. 5 - The transmission loss data of Fig. 4 smoothed in range. Each point represents the transmission loss of the average signal received over a range interval of 0.9 km.

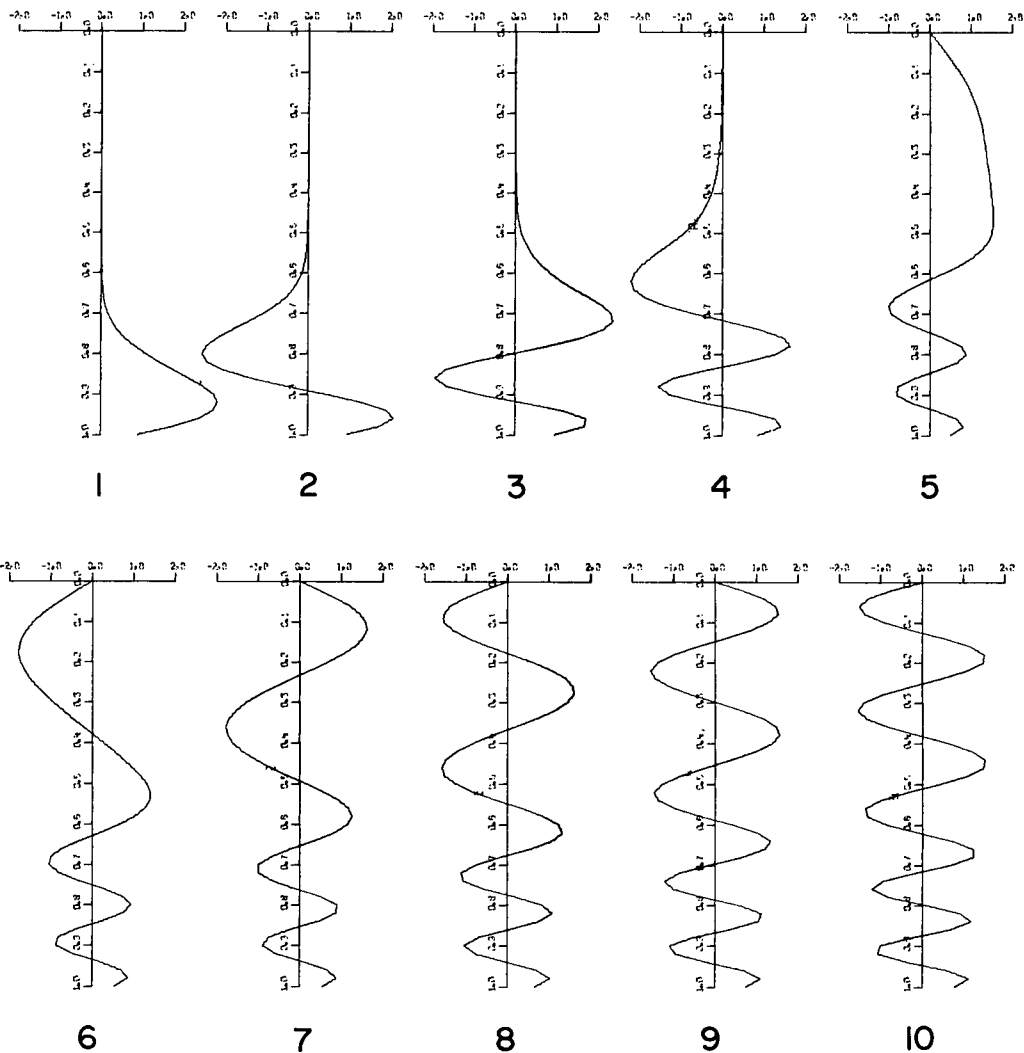


Fig. 6 - Normalized mode amplitude functions (eigenfunctions) for the ten lowest order modes predicted by the normal-mode computer program. The ordinate is depth normalized by the total water depth. The exponentially decreasing portions of the mode amplitude functions in the bottom are not shown.

From Eq. (1) it can be seen that unless a given mode amplitude has an appreciably nonzero value at the source depth, that mode will not be excited appreciably and will not contribute to the observed sound field. Since the source depth actually used was 15.2 m, corresponding to a normalized depth of 0.5, Fig. 6 indicates that the lowest order mode that should be significantly excited directly is the fourth. This is strictly true only for a point source. The chief effect of source directivity (or, equivalently, the fact that the source aperture of 3 m was fully $1/10$ of the water depth) is to inhibit the excitation of high-order modes. Knowledge of the eigenvalue for the mode (which is computed by the normal-mode program) and the speed of sound at the source depth allows one to compute the angle that the rays associated with a given mode make with the horizontal as they leave the source. Taking 5 degrees (the source half-angle at the 3-dB points) as the cut-off, it is found that the only modes whose associated rays leave the source within this angle are the modes of the twelfth and lower order.

Thus the model predicts that modes of lower order than the fourth and higher order than the twelfth should not be significantly excited. The distribution of received pressure over receiver depth is shown for several ranges in Fig. 7. Since the bottom slope is gentle, one would expect the modes to adapt "adiabatically" to the increasing depth, as has been observed in model experiments (Eby et al., 1960). The finding that at ranges greater than 15 km substantially more energy is near the surface than at the depth of the lowest hydrophone therefore shows that at these ranges the second and third modes are not dominant. Beyond 12 km the first-mode peak lies almost entirely at a lower depth than the lowest hydrophone; hence the presence of the first mode cannot be ruled out.

Since the effects that the excluded modes would have on the propagation can be estimated only qualitatively, it is not possible to relate these measurements of transmission loss to those that would be obtained, say, by an omnidirectional source in the sound channel.

CW Data

Fluctuations in amplitude and phase of signals received over a relatively fixed underwater path have been reported by many observers. By means of extensive observations of propagation over a fixed 74-naut-mi range, Weston et al. (1968), have identified ten

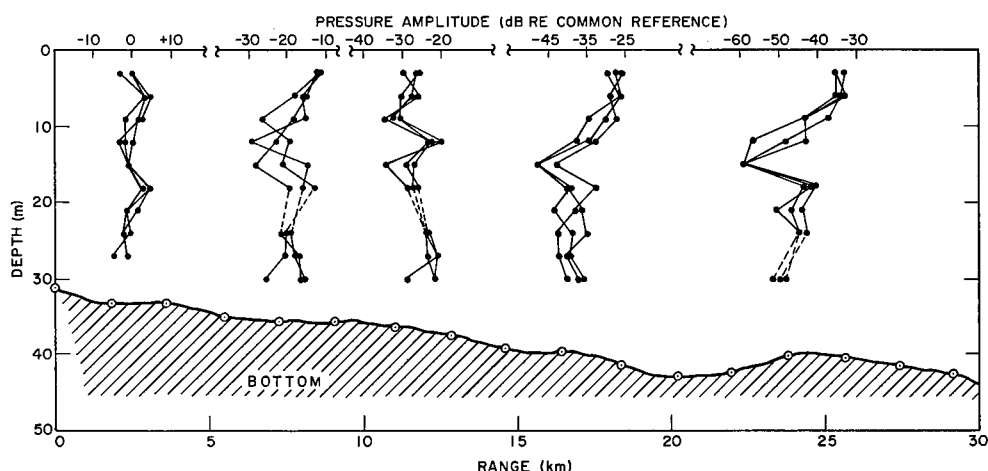


Fig. 7 - Distribution of received pressure amplitude with depth at ranges of 2.2, 7.3, 11.5, 16.8, and 25.3 km. At each range three successive pulses are plotted.

fluctuation mechanisms whose effects are noted on time scales ranging from 1 year (e.g. seasonal temperature changes) down to several seconds (surface waves). Much the same range of fluctuation has been observed over the Project MIMI 43-naut-mi path in somewhat deeper water in the Straits of Florida (Clark and Yarnall, 1967).

In shallow-water experiments in which the ratios of range to depth and depth to acoustic wavelength are comparable to the present experiment, pronounced fluctuations at surface-wave frequencies have been reported by Urick, Lund, and Bradley (1969), Scrimger (1961), Wood (1959) and Mackenzie (1962). Extreme sensitivity of the signal received at a fixed receiver to changes in water depth has been observed by Urick et al. (tidal variations of 2 feet in 60 feet of water) and Wood (evaporation of fractions of a millimeter of water in a model tank 50 mm deep).

The kinds of analysis that could be applied to the present data were limited in that the receiving hydrophones were not rigidly held. As indicated schematically in Fig. 2, the three hydrophones were suspended between a bottomed weight and a subsurface float and attached to the fantail of the ship by long electrical cables floating on the surface. The ship was anchored at the bow.

This design should have allowed almost no vertical motion of the array in response to the small surface waves observed (less than 0.6 m). However the array was constrained horizontally by only the weight at the bottom and the cables to the ship at the top. It was thus free to move horizontally (over a time scale of minutes) in response to currents. Since the acoustic wavelength (0.5 m) was small compared to possible horizontal motions, no analysis of the phase of the received signals was attempted.

In a normal-mode interference field, motion of the receivers can also affect the amplitude of the observed signal. Although detailed motion of the hydrophones is not known, it is thought that the only times when this motion was severe enough to influence the observed signal levels were the two occasions (once during each run) when the ship had swung enough that the electrical cables threatened to foul the anchor chain, necessitating the repositioning of the hydrophones about 200 m from their original location.

With these caveats in mind, the data were analyzed on three time scales: the time scale of the entire length of each run, during which effects of tidal motion might be observed; the time scale of minutes, during which evidence of internal waves would be expected; and the time scale of seconds, during which surface wave effects would be expected to predominate.

As a help in understanding the following description of these analyses, Appendix A gives some details of the digitization procedure and subsequent computer processing of the digital tapes.

Long-Period Fluctuations—The sound-speed profiles, as measured from velocimeter casts made periodically while the ship was anchored at each station, were generally similar for the two stations and relatively constant with time at each station. These profiles (Figs. 8a and 8b) consist of a nearly isovelocity layer for about the upper 15 m of the water column at 7.0 km and the upper 20 m at 27.6 km (at the larger range the water depth being approximately 10 m greater) and then of a sharp negative gradient to the bottom.

Plots of the signal amplitude received on the three hydrophones during the two anchored runs are presented in Figs. 9a and 9b. To produce these plots the digitized envelope-detected signals for the first 16 seconds of every 165-second digital record were averaged, converted to decibels, and then plotted as a function of time. Gaps in these graphs represent CW data lost due to various factors. There is a gap every 2 hr 20 min, during which analog tapes were calibrated and changed aboard the receiving ship.

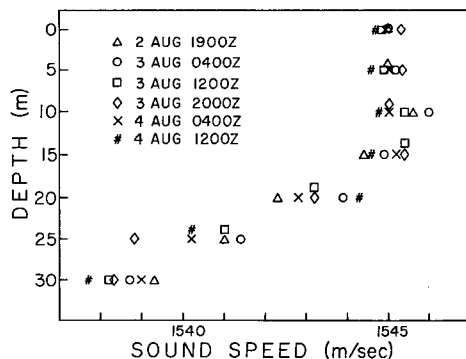


Fig. 8a - Sound-speed profiles measured by velocimeter casts during the 7.0-km anchored run

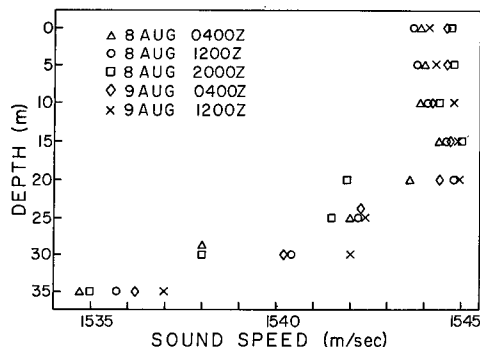


Fig. 8b - Sound-speed profiles measured by velocimeter casts during the 27.6-km anchored run

Other gaps were caused by instrumentation problems on the ship, on Stage I, or during digitization. The signal-to-noise ratio at the 27.6-km range can be observed on Fig. 9b, which shows the recorded levels when the source was turned off briefly near the end of the run.

Observed tides, which are strongly diurnal, are included in Figs. 9a and 9b. The plots in Fig. 9a suggest that during the 7.0 km run the acoustic amplitudes also varied with a diurnal period, but this would require more data to establish.

The general characteristics of the fluctuations observed in this experiment are similar to those reported by Weston et al. (1968) and Clark and Yarnall (1967). Both of these studies note that fluctuations of long period tend to affect the phase of the received signal much more markedly than its amplitude, whereas at shorter periods the amplitude fluctuations are dominant. Though of course phase fluctuations were not observed in this experiment, correspondence of amplitude fluctuations to the diurnal tidal period was weak. As will be seen later, the correspondence to surface-wave frequencies was much stronger. That the pronounced variation in amplitude at the tidal frequency observed by Urick, Lund, and Bradley (1969) was not observed here might be due to absence of the first three modes in the present case.

During the 7.0-km run the wind, surface waves, and swell were primarily from the east, with wind speeds averaging 10 knots and sea states from 0 to 2. At the 27.6-km range the winds were lighter and more variable in direction, with sea states 0 to 1. Wind and sea-surface data have not been included here, since they show no obvious correlation with the received signal amplitudes.

The same sets of points (each point an average of 16 seconds of data) used to generate the plots of Figs. 9a and 9b were also used to compute long-term coefficients of variation and crosscorrelation functions for the two runs. The coefficient of variation, a statistic frequently used in describing fluctuations, is defined as

coefficient of variation = standard deviation/mean

$$= \frac{\left(\frac{1}{N-1} \sum_i (x_i - \bar{x})^2 \right)^{1/2}}{\bar{x}}, \quad (2)$$

where the x_i 's are data points, \bar{x} is the mean, and N is the number of points in each summation. For this analysis the run was broken up into blocks 3 hours long, over which

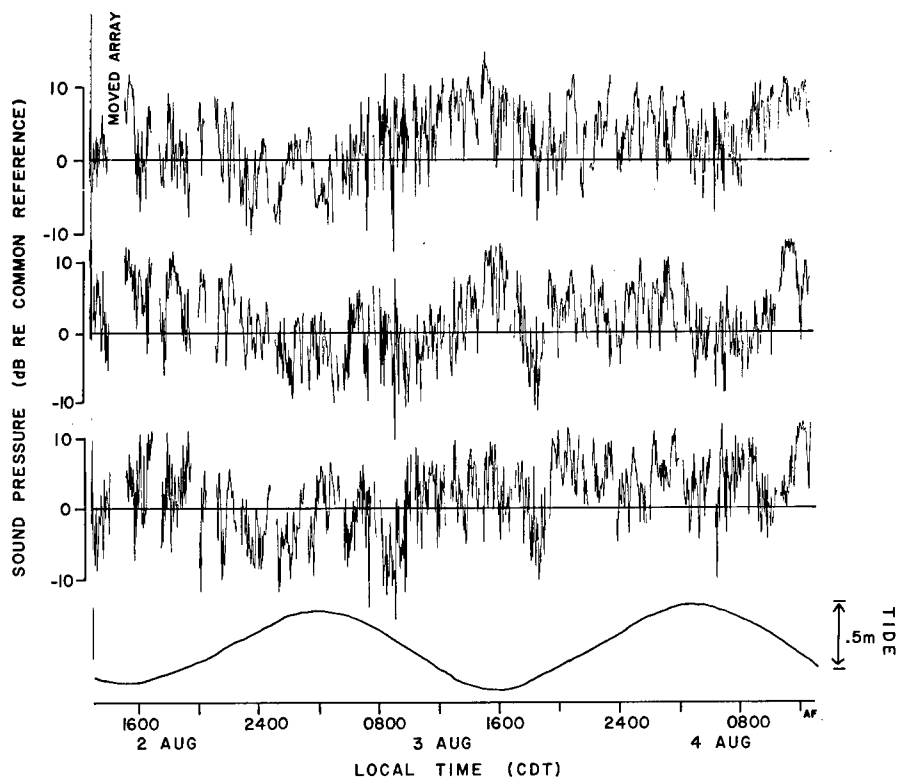


Fig. 9a - Signal amplitudes received during the 7.0-km anchored run. Starting at the top, the four time series shown are the signals from the upper, middle, and lower hydrophones and the observed tide.

UNCLASSIFIED

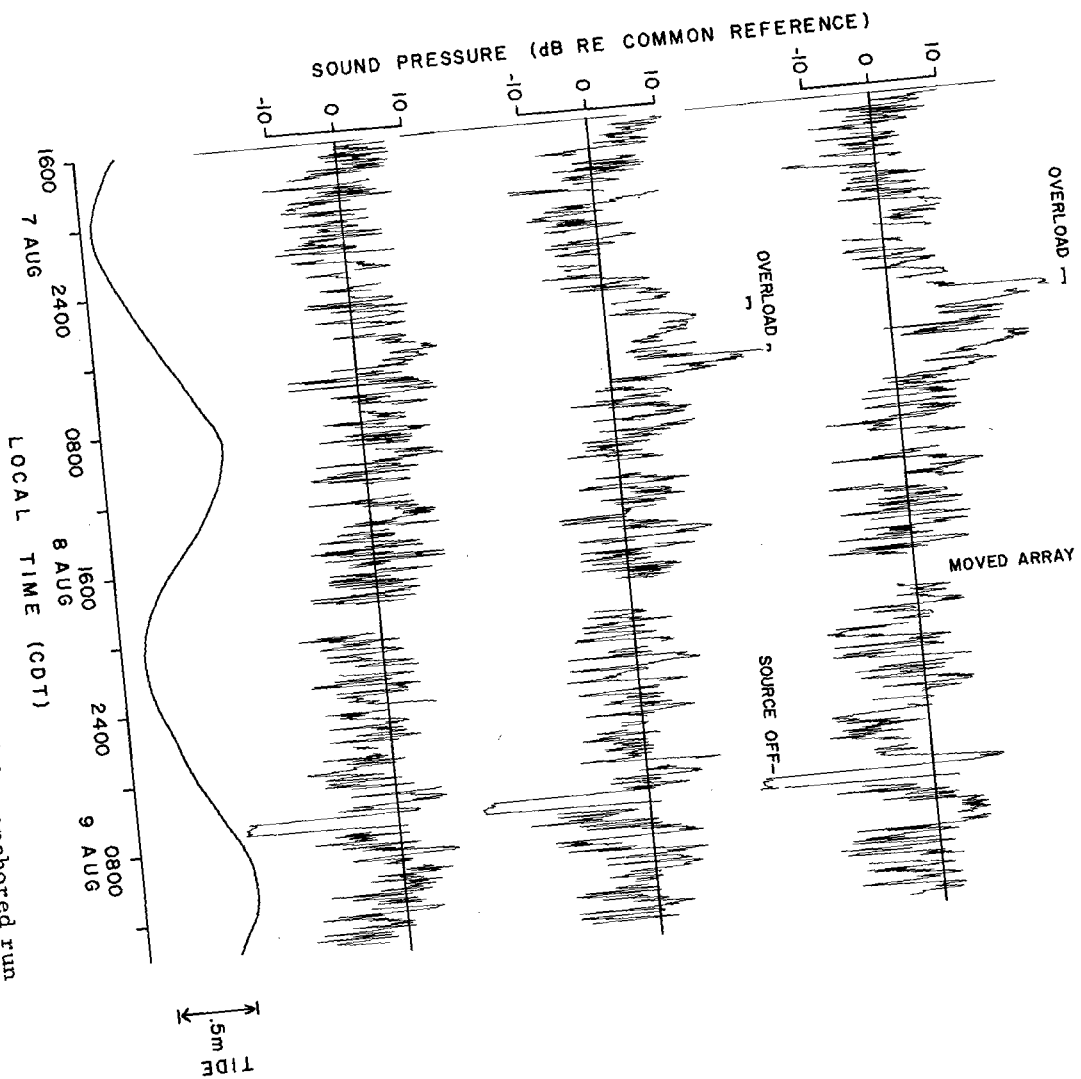
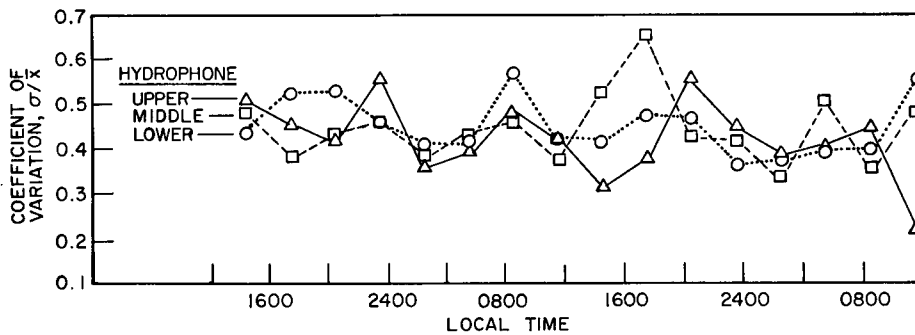
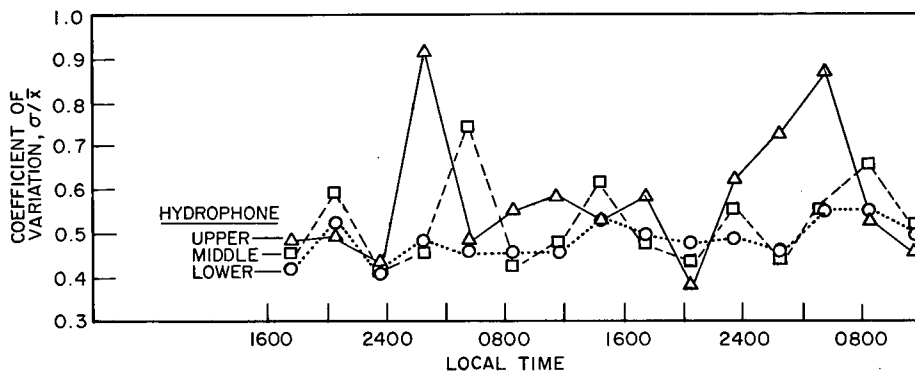


Fig. 9b - Same as Fig. 9a, but for the 27.6-km anchored run

the statistics are assumed to be roughly stationary. Each data block contained from 35 to 64 data points, depending on the occurrence of gaps within the block. The sums in Eq. (2) thus run over each such 3-hour block. The results are plotted in Fig. 10. There are no periods of exceptionally steady signals (low coefficients of variation), and the two peaks on the upper hydrophone at 27.6 km appear to be due mainly to nonstationarity of the received signal within those 3-hour blocks. The average values of the coefficients of variation are 0.44 at 7.0 km and 0.55 at 27.6 km.



(a) 7.0-km run



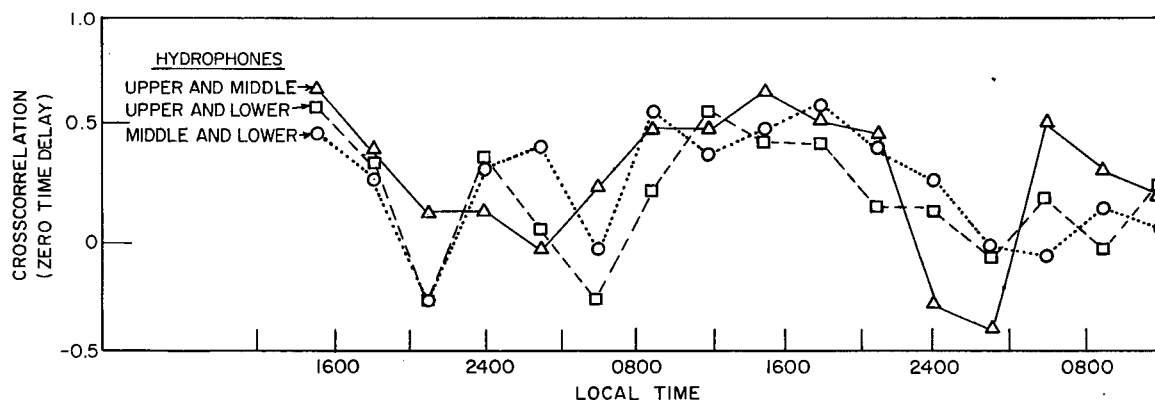
(b) 27.6-km run

Fig. 10 - Coefficients of variation as a function of time for the two anchored runs. Each point represents 3 hours of data.

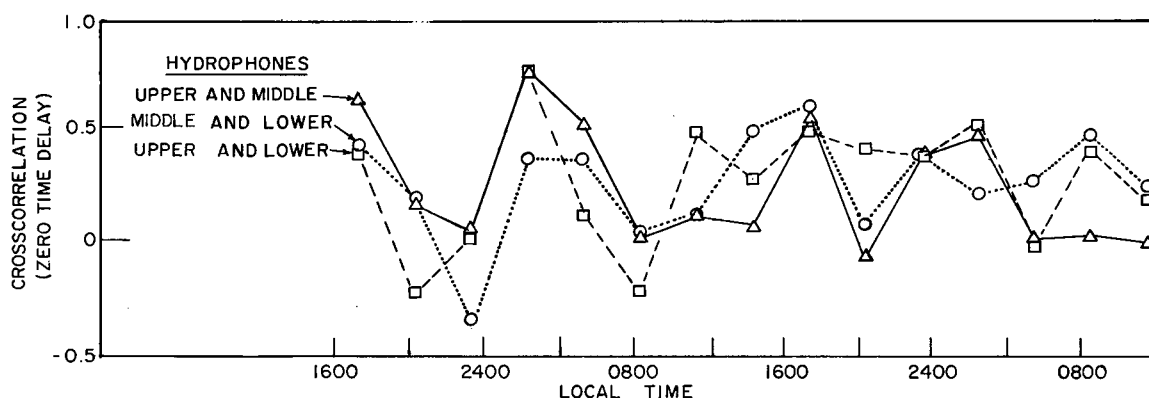
The crosscorrelation coefficient C_{xy} , at zero time delay, between hydrophones x and y is defined (Bendat and Piersol, 1966, pp. 298-299) as

$$C_{xy} = \frac{\sum (x_i - \bar{x}) (y_i - \bar{y})}{\left[\sum (x_i - \bar{x})^2 \sum (y_i - \bar{y})^2 \right]^{1/2}} \quad (3)$$

where again the sums are taken over the same 3-hour data blocks. The crosscorrelation coefficients are shown in Fig. 11. Most of the crosscorrelation coefficients between any two of the three hydrophones lie between 0 and 0.5. No structure is observed



(a) 7.0-km run



(b) 27.6-km run

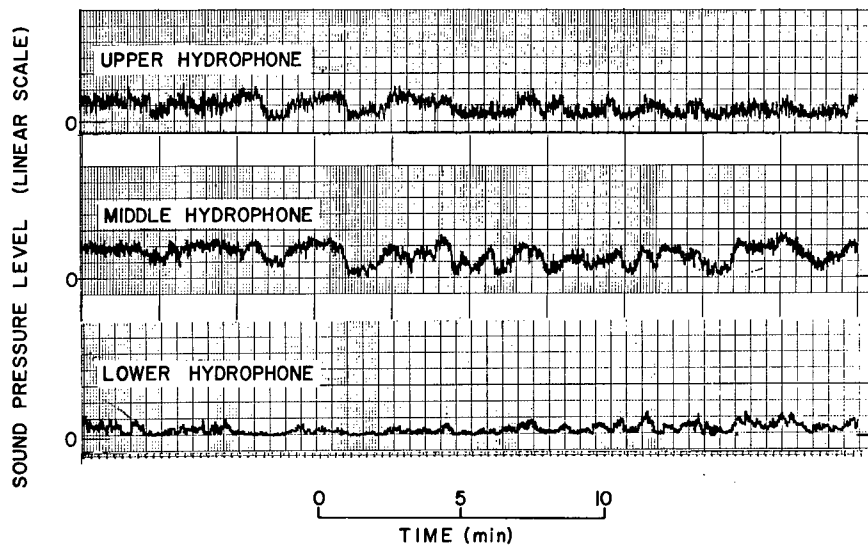
Fig. 11 - Crosscorrelation coefficients (at zero time delay) as a function of time for the two anchored runs. Each point represents 3 hours of data.

in the crosscorrelation coefficient as a function of time for the 27.6-km run, but at 7.0 km the curves seem to be oscillating with a period of about 1 day (the tidal period).

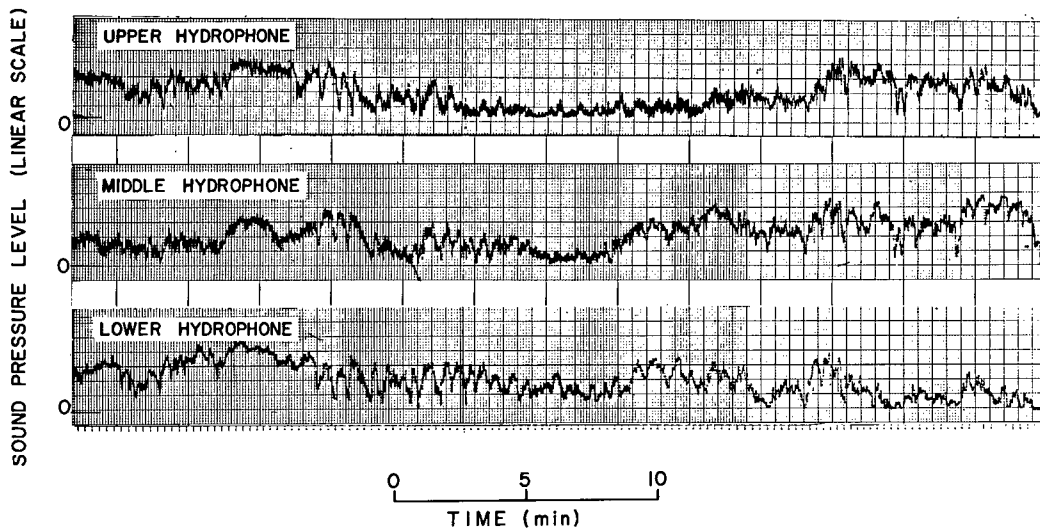
Medium-Period Fluctuations—Quasi-regular fluctuations in signal amplitude at periods ranging from about 30 sec up to 30 min can be observed in about 20% of the data taken at the two anchored stations. Figure 12a shows an example of the signals received at the 7.0-km range (August 3, 1600-1625 CDT). Fluctuations with a period of several minutes are evident, especially on the middepth hydrophone. Figure 12b is a sample from the 27.6-km range (August 8, 0940-1020 CDT); here superposed on slower variations are observed quite striking fluctuations with a period of about 30 seconds.

There are several possible explanations for these phenomena, none of which can be positively identified without more environmental data than is available. Weston et al. (1968), for example, list seven possible fluctuation mechanisms for periods of the order of minutes, of which they have been able to observe directly only two: short-term random changes in fish aggregation and internal waves.

Short-Period Fluctuations—As mentioned, fluctuations in the received signal level over a time span of seconds have been reported many times in the literature. Such fluctuations occur throughout the present data; an example is shown in Fig. 13, which is



(a) Example at the 7.0-km range



(b) Example at the 27.6-km range

Fig. 12 - Examples of the medium-period fluctuations observed at the two ranges of anchored runs

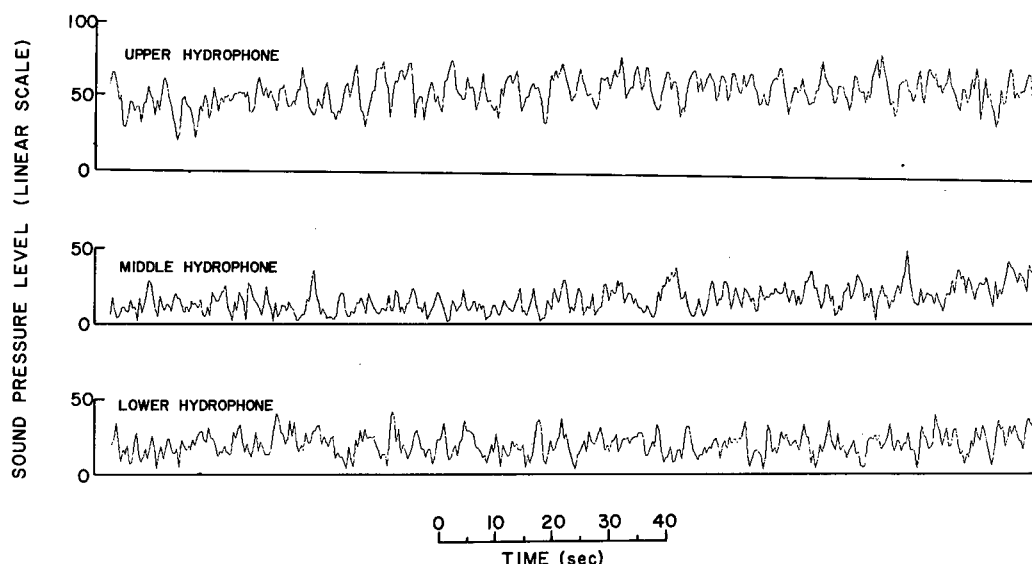


Fig. 13 - An example of the received amplitudes at 7.0 km, showing pronounced fluctuations with periods of a few seconds

a computer plot of the detected signal level during one data record (163 seconds) of tape 107, recorded at the 7.0-km range at 0330 local time on August 3, 1968. Rapid fluctuations are clearly visible in all three channels in this figure.

In an effort to determine more precisely the dominant frequencies of fluctuation, power spectra were obtained from each analog tape. The power spectrum made from data records 2-7 of tape 107 (this includes the data record of Fig. 13) is shown in Fig. 14. In finding the maximum level used to normalize the spectrum, the three lowest-frequency estimates (0 Hz, 0.012 Hz, and 0.024 Hz) were omitted, since they tend to be 20 dB above the rest of the spectrum (the zero frequency component, for example, is proportional to the square of the mean value of the time series). Appendix B further discusses the procedure used to obtain these spectra, confidence limits on the spectral estimates, and possible aliasing of the spectra.

Figure 14 shows that the fluctuations observed in Fig. 13 are peaked about two dominant frequencies, 0.12 Hz (period $T = 8.5$ sec) and 0.24 Hz ($T = 4$ sec). Although direct measurements were not made on the surface waves, the wind waves and swell were both observed on the ship to be about 1 foot high. It is known that the most common wave periods in this area are between 4 and 6 seconds, with swell periods slightly longer (Tolbert and Austin, 1959), so it seems reasonable to assign the two peaks at 0.12 Hz and 0.24 Hz to the influence of swell and wind waves respectively.

In a similar fashion, spectra were taken of the second through seventh data records of each of the analog tapes. Most of these spectra display the same general characteristics as shown in Fig. 14. These features are (a) a sharp peak at about 0.24 Hz, (b) frequently another peak at about 0.12 Hz, and (c) spectral levels for all three channels which are very nearly equal, especially at the frequencies of the major peaks in the spectrum.

The two series of spectra thus obtained at each range are shown in Fig. 15 for the upper hydrophone only. In this figure all the spectra at each range have been normalized to the same power level. Each cut represents the spectrum from a different analog tape; there is an interval of about 2 hr 20 min between successive cuts.

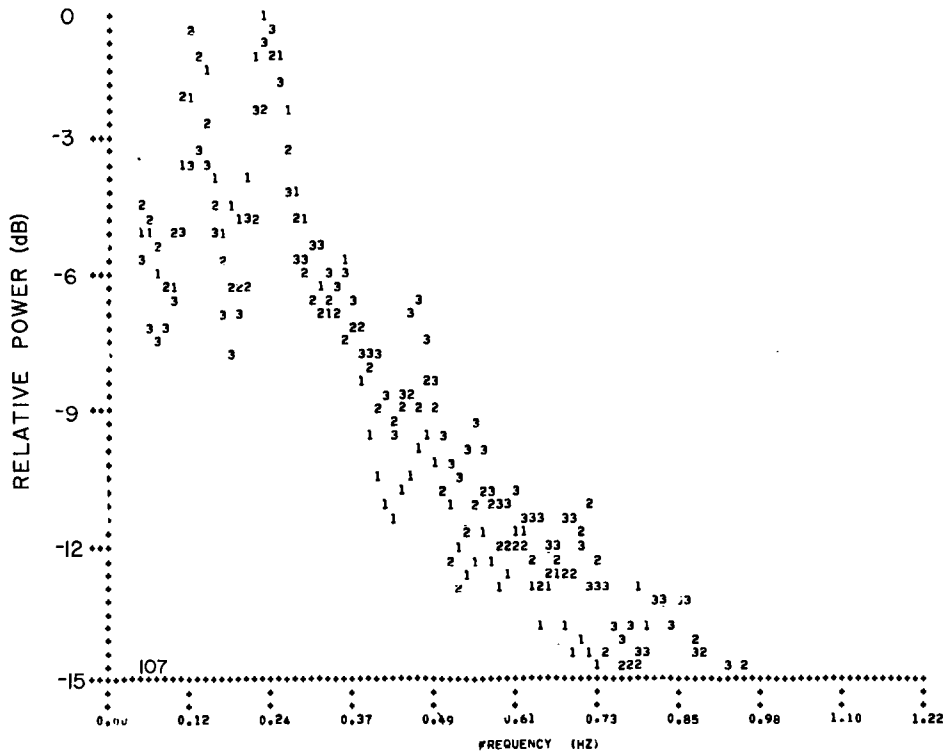
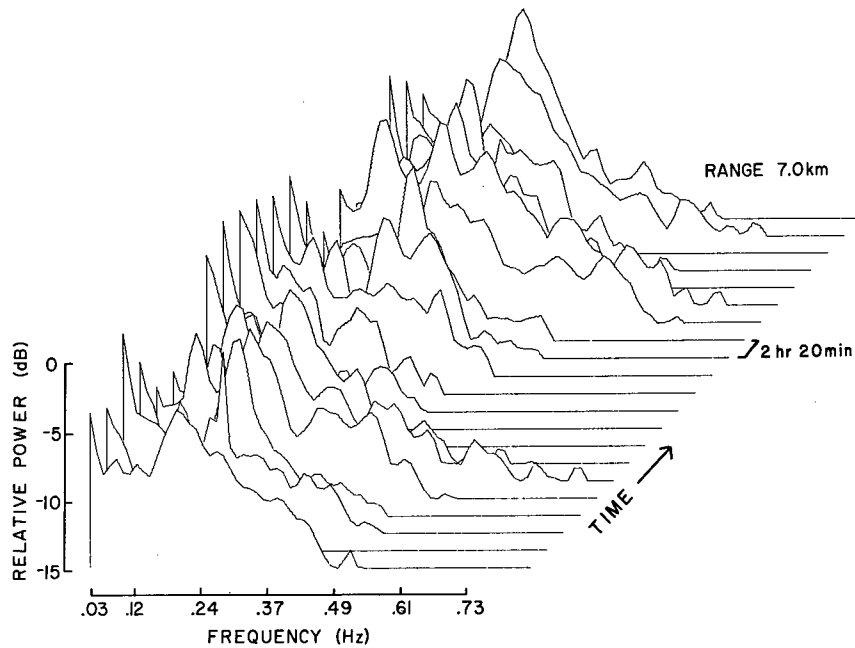


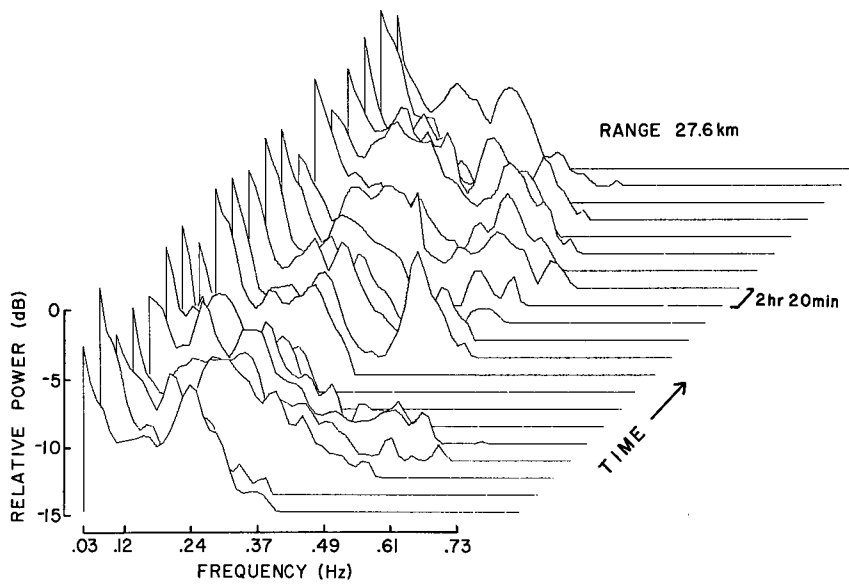
Fig. 14 - Power spectrum of the received signal amplitudes at 7.0 km over a time span that includes the record shown in Fig. 13. Plotted above frequency values 0.012 Hz apart are the numerals 1, 2, and 3, referring respectively to the upper, middle, and lower hydrophones.

The most obvious difference between the two series of spectra in Fig. 15 is that the peaks from 0.12 to 0.24 Hz in the 7.0-km data have a greater height relative to the lower frequency spectral levels than those in the 27.6-km data. As mentioned, wave and swell conditions were generally similar during the two runs, with slightly higher wind waves at the shorter range. The results of Scrimger (1961) suggest that at the wave heights and signal frequency of this experiment, amplitude fluctuations of this time scale would be caused mainly by surface waves near the source or the receiver but not in between. If this is the case, the effect of surface waves would not be expected to vary with range per se. The observed difference might then be caused by changes in the mode structure with range or by the difference in wave heights.

One feature that should be noted in some of the power spectra is a substantial additional peak in the vicinity of 0.4 Hz. This first shows up strongly in the tenth spectrum of Fig. 15b (27.6-km range). This spectrum is shown in Fig. 16, where it can be seen that the assumed surface-wave peaks have moved to slightly lower frequency (about 0.16 and 0.21 Hz) and that this new peak is at approximately their second harmonic frequency. Fluctuations at the second harmonic of the surface-wave frequency were observed by Scrimger (1961) when the ratio of acoustic wavelength to crest-to-trough wave height was greater than about 18. The same effect may be occurring in the present case, although the waves at the time were estimated to have a crest-to-trough height of up to 15 cm. For several hours previously there had been almost no observable wave action; hence there were probably also present at this time a number of rather smaller waves, caused by the gradual increase in wind speed.



(a) 7.0-km range



(b) 27.6-km range

Fig. 15 - Power spectra (upper hydrophone only) as a function of time. Each spectrum represents about 16 min of data, and there is a gap of 2 hr 20 min between successive spectra.

Appendix A

DIGITIZATION AND COMPUTER PROCESSING

The purpose of this appendix is to elaborate on the analog-to-digital conversion procedure employed with the CW data and to describe some of the computer manipulations required to get the resulting data into useful form.

DIGITIZATION

As was mentioned in the section "NRL Processing," the analog data were played back at 60 ips, were envelope-detected, and were digitized using a 10-bit-plus-sign analog-to-digital converter controlled by the NAREC computer. Because the input range of the converter was approximately -9.5 volts to +9.5 volts, the detected signals were passed through operational amplifiers to change their range of 0 to 2 V dc to -8 to +8 V dc. This allowed almost the full range of the analog-to-digital converter (2^{11} or 2048 steps) to be used, thus permitting excellent digital resolution. Since the NAREC and the CDC 3800 computers both use 48-bit words, as many as four digital samples could have been packed into one computer word. However, to facilitate channel identification, only three digital samples (one each from the upper, middle, and lower hydrophones) were put into each computer word. Check bits were used to ensure that a loss of digitizer channel synchronization could be detected during subsequent computer processing of the digitized data.

The data were written out on tape in 2048-word records. The first two words of each record contained in coded form the time at the start of the record (hours, minutes, and seconds) taken from the time-code channel recorded on the analog tapes, the original analog tape number, and a flag bit indicating whether the rest of the record consisted of a calibration signal or received hydrophone signals. Calibration ladders spanning 40 dB were placed at the beginning and end of each analog tape. These were sampled at a rate of 400 samples of each channel per second (since the tape was being played back at 16 times the speed it was recorded, this gave a real time sampling rate of 25 per second); data records were sampled at 200 per second (real time rate 12.5 per second). Approximately 16 analog tapes could be accommodated on one digital tape.

BACKGROUND PROCESSING

After the digital tapes were recorded, they were checked for parity errors, short records, and the like using the CDC 3800 Utility routine. One analog tape was found to have many parity errors and had to be redigitized. During subsequent processing it was found that when parity errors occurred during tape reading, the fault was invariably with the tape transport, not with the input tape.

Subroutines Decode and Convert were written in the CDC assembly language Compass to allow calibration records to be printed out. Subroutine Decode looks at the first two words of a record and determines from them the time, the tape number, and whether the record contains data or calibration signals. Subroutine Convert checks the synchronization bits and unpacks the three data samples from each word, converts from the sign-plus-magnitude number system of the NAREC to the 1's complement system of the CDC 3800, converts to CDC floating point form, then finally multiplies by a constant to recover dc voltage into the analog-to-digital converter.

The calibration ladders, each of which consists of 20 2-dB voltage steps inserted in place of the hydrophone voltages at the beginning and end of each analog tape, were read manually to establish a linear equation relating output voltage of the hydrophone to voltage into the digitizer for each channel of each tape. Another Compass routine, Calib, was then used to apply these equations (and the known hydrophone sensitivities) to the output of the Convert subroutine; the resulting data values in terms of dynes/cm² sound pressure level were then used in all further processing.

Appendix B

POWER SPECTRUM TECHNIQUES

This appendix presents further details on the power spectrum techniques employed in the analysis of the CW data.

ALIASING

Whenever data are sampled at a constant frequency f_s , the problem of aliasing arises (Bendat and Piersol, 1966, pp. 278-280), because power at frequencies $nf_s \pm f$, $n = 1, 2, \dots$, is folded back into the spectral estimate at the frequency f . Thus, if there is a large concentration of power near the sampling frequency f_s or its harmonics, this will appear as spurious low-frequency power in the spectrum. In the present case the power spectral density was observed to decrease smoothly with frequency from about 0.5 Hz up to the Nyquist frequency $f_s/2$ (6.25 Hz), which is the highest frequency for which one obtains spectral data. Since in all instances the power level near the Nyquist frequency was about 40 dB below that at the low frequencies of interest, it is concluded that aliasing was negligible.

TRANSFORM METHOD

The classic method of producing power spectra, described in detail by Blackman and Tukey (1959), is to form the autocorrelation function of the original time-series data and then to take a cosine transform of the autocorrelation weighted with a suitable lag window. However, with the advent of the fast Fourier transform (FFT) algorithm (Cooley and Tukey, 1965), it has become more convenient to obtain power spectra by direct application of the discrete Fourier transform; this is the method that was used in the present work. A useful exposition of this method of obtaining spectra has been given by Hinich and Clay (1968), which contains more details than are given below.

Consider a stationary discrete process sampled at time intervals of Δ . Given a finite record X_0, \dots, X_{n-1} of these data samples, with $X_r = X(r\Delta)$, applying the FFT yields n complex Fourier coefficients A_k , where

$$A_k = \left(\frac{\Delta}{n}\right)^{1/2} \sum_{r=0}^{n-1} X_r e^{2\pi i k(r/n)}, \quad k = 0, 1, \dots, n-1, \quad (\text{A1})$$

Hinich and Clay show that the term $|A_k|^2$ is an estimate of the true power spectral density of the process around the frequency $f_k = k/n\Delta$ (neglecting aliasing). Since from Eq. (A1) $A_k = A_{n-k}^*$, where A_{n-k}^* is the complex conjugate of A_{n-k} , it follows that $|A_k|^2 = |A_{n-k}|^2$, so there are $n/2$ power spectral estimates generated in this way. For all of the figures presented here, $n = 1024$ points were used in the time series. Thus the frequency spacing of the spectral estimates is

$$\frac{1}{n\Delta} = \frac{1}{1024 \times 0.08 \text{ sec}} = 0.012 \text{ Hz}.$$

Unless some form of smoothing is used, each spectral estimate is highly uncertain; in fact, depending on the exact nature of the input data, if power spectra are obtained from

different data records drawn from the same stationary process, the variance of any of the $|A_k|^2$ values can be as much as 100% of its mean value (Hinich and Clay, 1968). There are basically two ways to reduce the variance: by averaging several spectra and by smoothing over adjacent frequency estimates. In the present work both methods were applied. The procedure was as follows:

1. Six contiguous 2046-point data records were selected and extended to 2048 points each. Each record was then split in half, and a power spectrum $\{|A_k|^2\}_i, i = 1, \dots, 12$, computed for each of the 12 resulting 1024-point blocks. The variance s_i^2 of each block was also computed.

2. The twelve spectra were averaged point by point:

$$|A_k|_{av}^2 = \frac{1}{12} \sum_{i=1}^{12} |A_k|_i^2.$$

3. The averaged spectrum was then hanned, or smoothed over adjacent frequency estimates, using

$$G_k = 0.5 |A_k|_{av}^2 + 0.25 \left(|A_{k-1}|_{av}^2 + |A_{k+1}|_{av}^2 \right), \quad k > 1.$$

4. For each channel the variances s_i^2 computed for the 12 data blocks were averaged, and the smoothed spectrum $\{G_k\}$ was divided by the averaged variance. Since the variance is merely the total fluctuation power of the input series $\{x\}$ (Jenkins and Watts, 1968), this scales the three channels (which may have differing amounts of power in the fluctuations) so that they can be plotted on the same scale.

CONFIDENCE LIMITS ON THE SPECTRAL ESTIMATES

One can obtain a rough feeling for the statistical accuracy of the resulting spectrum by making the usual assumption that the spectral estimates G_k are distributed about the true power spectrum with a chi-squared distribution. Applying a formula derived on this assumption by Blackman and Tukey (1959, p. 149), one finds that in the present case each spectral estimate should fall within an interval of about 3 dB 90% of the time.

REFERENCES

- Bendat, J.S., and Piersol, A.G. (1966), Measurement and Analysis of Random Data (Wiley, New York)
- Blackman, R.B., and Tukey, J.W. (1959), The Measurement of Power Spectra (Dover, New York)
- Clark, J.G., and Yarnall, J.R. (1967), "Long Range Ocean Acoustics and Synoptic Oceanography—Straits of Florida Results," in Proceedings of the 4th U.S. Navy Symposium on Military Oceanography, Vol. I, pp. 309-365
- Cooley, J.W., and Tukey, J.W. (1965), "An Algorithm for the Machine Calculation of Complex Fourier Series," Math Computation 19, 297-301
- Eby, R.K., Williams, A.O., Jr., Ryan, R.P., and Tamarkin, P. (1960), "Study of Acoustic Propagation in a Two-Layered Model," J. Acoust. Soc. Amer. 32, 88-99
- Ferris, R.H., Ingenito, F., and Faber, A.L. (1970), "Experimental Separation and Identification of Acoustic Normal Modes in Shallow Water," NRL Report 7174
- Ferris, R.H., and Kuperman, W. (1970), "An Experiment on Acoustic Reflection from the Sea Surface," NRL Report 7075, p. 12
- Gregory, J.B. (1969), "Performance Characteristics of a Parabolic and a Conical Underwater Acoustic Reflector," NRL Report 6817
- Hinich, M.J., and Clay, C.S. (1968), "The Application of the Discrete Fourier Transform in the Estimation of Power Spectra, Coherence and Bispectra of Geophysical Data," Reviews of Geophysics 6, 347-363
- Jenkins, G.M., and Watts, D.G. (1968), Spectral Analysis and its Applications (Holden-Day, San Francisco), pp. 217-218
- Mackenzie, K.V. (1962), "Long-Range Shallow-Water Signal-Level Fluctuations and Frequency Spreading," J. Acoust. Soc. Amer. 34, 67-75
- Scrimger, J.A. (1961), "Signal Amplitude and Phase Fluctuations Induced by Surface Waves in Ducted Sound Propagation," J. Acoust. Soc. Amer. 33, 239-247
- Tolbert, W.H., and Austin, G.B. (1959), "On the Nearshore Marine Environment of the Gulf of Mexico at Panama City, Florida," U.S. Navy Mine Def. Lab., Panama City, Fla., Technical Paper TP161, p. 49
- Tolstoy, I., and Clay, C.S. (1966), Ocean Acoustics (McGraw-Hill, New York)
- Urlick, R.J., Lund, G.R., and Bradley, D.L. (1969), "Observations of Fluctuation of Transmitted Sound in Shallow Water," J. Acoust. Soc. Amer. 45, 683-690
- Weston, D.E., Horrigan, A.A., Thomas, S.J.L., and Revie, J. (1968), "Studies of Sound Transmission Fluctuations in Shallow Coastal Waters," Admiralty Research Laboratory, Teddington, Middlesex, ARL/L/R69
- Wood, A.B. (1959), "Model Experiments on Sound Propagation in Shallow Seas," J. Acoust. Soc. Amer. 31, 1213-1235

Security Classification		DOCUMENT CONTROL DATA - R & D	
(Security classification of title, body of abstract and indexing annotation must be entered when the overall report is classified)			
1. ORIGINATING ACTIVITY (Corporate author)		2a. REPORT SECURITY CLASSIFICATION	
Naval Research Laboratory Washington, D. C. 20390		Unclassified	
		2b. GROUP	
3. REPORT TITLE			
AN EXPERIMENT ON TRANSMISSION LOSS AND FLUCTUATIONS OF 3-kHz SOUND IN SHALLOW WATER			
4. DESCRIPTIVE NOTES (Type of report and inclusive dates) This is a final report on two NRL Problems. Problem S01-33 is closed, NRL Problem S01-45 is continuing.			
5. AUTHOR(S) (First name, middle initial, last name)			
Andrew L. Faber			
6. REPORT DATE		7a. TOTAL NO. OF PAGES	7b. NO. OF REFS
April 13, 1971		30	17
8a. CONTRACT OR GRANT NO.		9a. ORIGINATOR'S REPORT NUMBER(S)	
NRL Problems S01-33 and S01-45		NRL Report 7257	
b. PROJECT NO.			
RF 05-552-401-5257 and			
RF 05-552-404-5350			
c. SF 11-552-001-8621 and		9b. OTHER REPORT NO(S) (Any other numbers that may be assigned this report)	
d. SF 11-552-001-14275			
10. DISTRIBUTION STATEMENT			
Approved for public release; distribution unlimited.			
11. SUPPLEMENTARY NOTES		12. SPONSORING MILITARY ACTIVITY	
		Department of the Navy (Naval Ship Systems Command, Washington, D.C. 20360 and Office of Naval Research, Arlington, Virginia 22217)	
13. ABSTRACT			
<p>This experiment investigated certain aspects of the 3-kHz sound field produced by a source at middepth in shallow water off Panama City, Florida. The sound-speed profile consists of a weak surface channel in the upper half of the water column and a strong negative gradient in the lower half. A two-layer normal-mode model predicts that due to the source placement and high directivity, modes of lower order than the fourth or higher order than the twelfth should not be significantly excited. The prediction concerning the absence of the second and third modes tends to be supported by the amplitude distribution over depth observed at ranges of 15 to 27 km during a towed-hydrophone run (the data are inconclusive concerning the first mode). In the second part of the experiment the anchored receiving ship recorded about 48 hours of CW signals at each of two ranges: 7.0 km and 27.6 km. Over the total time span of the data the amplitude fluctuations of signals received on three hydrophones at different depths were observed to be weakly correlated, and there was some indication of variation at the tidal frequency for the 7.0-km data. On a shorter time scale, semiperiodic fluctuations at periods from 30 sec to 30 min occurred at times during these runs. Spectra of the signal amplitudes display strong peaks at the surface wave and swell frequencies, with the effect being somewhat greater at the shorter range, and with all three hydrophones having at any time similar fluctuation spectra.</p>			

14. KEY WORDS	LINK A		LINK B		LINK C	
	ROLE	WT	ROLE	WT	ROLE	WT
Underwater acoustics Shallow water Transmission loss Fluctuations 3-kHz sound Normal modes						